

Research
Engines and Fuels—Article

Injection Strategy in Natural Gas–Diesel Dual-Fuel Premixed Charge Compression Ignition Combustion under Low Load Conditions

Hyunwook Park, Euijoon Shim, Choongsik Bae *

Department of Mechanical Engineering, Korea Advanced Institute of Science and Technology (KAIST), Daejeon 34141, Republic of Korea



ARTICLE INFO

Article history:

Received 14 April 2018

Revised 12 November 2018

Accepted 18 March 2019

Available online 26 April 2019

Keywords:

Dual fuel

Reactivity controlled compression ignition

Premixed charge compression ignition

Natural gas

Injection strategy

Exhaust gas recirculation

ABSTRACT

Dual-fuel premixed charge compression ignition (DF-PCCI) combustion has been proven to be a viable alternative to conventional diesel combustion in heavy-duty compression ignition engines due to its low nitrogen oxides (NO_x) and particulate matter (PM) emissions. When natural gas (NG) is applied to a DF-PCCI engine, its low reactivity reduces the maximum pressure rise rate under high loads. However, the NG–diesel DF-PCCI engine suffers from low combustion efficiency under low loads. In this study, an injection strategy of fuel supply (NG and diesel) in a DF-PCCI engine was investigated in order to reduce both the fuel consumption and hydrocarbon (HC) and carbon monoxide (CO) emissions under low load conditions. A variation in the NG substitution and diesel start of energizing (SOE) was found to effectively control the formation of the fuel–air mixture. A double injection strategy of diesel was implemented to adjust the local reactivity of the mixture. Retardation of the diesel pilot SOE and a low fraction of the diesel pilot injection quantity were favorable for reducing the combustion loss. The introduction of exhaust gas recirculation (EGR) improved the fuel economy and reduced the NO_x and PM emissions below Euro VI regulations by retarding the combustion phasing. The combination of an NG substitution of 40%, the double injection strategy of diesel, and a moderate EGR rate effectively improved the combustion efficiency and indicated efficiency, and reduced the HC and CO emissions under low load conditions.

© 2019 THE AUTHORS. Published by Elsevier LTD on behalf of Chinese Academy of Engineering and Higher Education Press Limited Company. This is an open access article under the CC BY-NC-ND license (<http://creativecommons.org/licenses/by-nc-nd/4.0/>).

1. Introduction

Global carbon dioxide (CO_2) emissions from transportation have been increasing for decades, with light-duty and heavy-duty vehicles accounting for most of these emissions. Therefore, significant efforts are needed to improve vehicle efficiency to reduce the CO_2 emissions in road transportation [1]. Diesel engines have contributed to transportation because of their high fuel efficiency and torque. However, diesel engines today must meet stringent emissions regulations, especially in regards to nitrogen oxides (NO_x) and particulate matter (PM) emissions. The implementation of after-treatment systems is necessary to meet the Euro VI regulation for diesel engines. However, such implementation increases the vehicle cost and fuel consumption [2]. Although the adoption of after-treatment systems is effective in meeting the Euro VI requirement, due to the high cost of these systems, lowering the

exhaust emissions of diesel engines should be achieved through the development of combustion technologies.

Various types of in-cylinder combustion technologies in diesel engines have been developed to reduce NO_x and PM emissions. These technologies include homogeneous charge compression ignition, premixed charge compression ignition (PCCI), and low temperature combustion. In terms of advantages, these technologies effectively suppress NO_x and PM emissions because a locally leaner premixed fuel–air mixture reduces the combustion temperature in comparison with that of conventional diesel combustion (CDC) [2–5]. The thermal efficiency is improved by the reduced combustion duration of the premixed fuel–air mixture and the lower heat transfer loss of the low combustion temperature, compared with that of CDC [2]. However, the following challenges must still be overcome in order to commercialize these technologies in diesel engines: Control of combustion phasing is difficult over a wide range of speeds and loads because the auto-ignition is influenced by chemical kinetics [3]. The engine operating range is limited with these technologies. In low load operations, hydrocarbon (HC) and carbon monoxide (CO) emissions increase

* Corresponding author.

E-mail address: csbae@kaist.ac.kr (C. Bae).

significantly as a result of incomplete combustion [4]. In high load operations, the sudden heat release of the premixed fuel–air mixture results in a high level of maximum pressure rise rate (MPRR), which induces significant combustion noise and even engine damage [5].

Dual-fuel PCCI (DF-PCCI), which includes dual-fuel combustion and reactivity controlled compression ignition (RCCI) combustion, presents a possible solution to the challenges affecting in-cylinder combustion technologies, as described above. DF-PCCI is a dual-fuel combustion technology that employs in-cylinder fuel blending with two fuels of different reactivity [6,7]. Typically, a low-reactivity (high octane number) fuel is introduced during the intake stroke or early compression stroke to create a premixed fuel–air mixture, and then a high-reactivity (high cetane number) fuel—usually diesel—is directly injected into the combustion chamber. The combustion phasing in the DF-PCCI concept can be controlled by the blending ratio of the two fuels, the injection timing of the high-reactivity fuel, and the exhaust gas recirculation (EGR) rate [8–10]. A great deal of research on the DF-PCCI concept has been conducted with gasoline and diesel in order to make use of the existing infrastructure. For the DF-PCCI concept with gasoline and diesel, it has been demonstrated that the engine load can be operated from low to high loads [11–18]. At low load operation, the diesel portion in the fuel–air mixture increases to improve combustion efficiency [11–13]. However, as the engine operation is moved to high loads, a higher gasoline portion in the fuel–air mixture and a higher EGR rate should be applied to reduce the MPRR. In the DF-PCCI concept, the peak heat release rate (HRR) can be reduced by equivalent ratio and reactivity stratification, which results in the staged consumption of the two fuels [14]. In this way, the MPRR can be suppressed successfully. However, low load operation in the DF-PCCI concept still suffers from high levels of HC and CO emissions, as well as degradation of thermal efficiency [14,15]. High load operation is also limited by high levels of peak pressure and MPRR, despite the wider high load range in comparison with that of in-cylinder combustion technologies [16–18].

Natural gas (NG) has recently been considered to be an attractive option in heavy-duty transport applications, mainly because of its competitive price and low carbon-to-hydrogen ratio [19,20]. When NG is applied to the DF-PCCI concept, the engine can be operated at a higher load condition with reduced MPRR; this is because the octane number of NG is higher than that of gasoline, resulting in a larger difference in the reactivity gradient between NG and diesel than between gasoline and diesel [21–23]. Walker et al. [21] introduced methane in a DF-PCCI engine to assess the expansion of the operating range over gasoline. When methane was applied to the DF-PCCI concept, the engine operated at a higher load compared with the gasoline–diesel DF-PCCI concept, because the combustion duration was relatively wider in the DF-PCCI engine with methane. The lower reactivity of the methane extended the combustion duration, which reduced the peak MPRR at high load operation. An experimental investigation by Dahodwala et al. [22] indicated that the engine operated at a 1.4 MPa brake mean effective pressure (BMEP) with the NG–diesel DF-PCCI mode. Diesel double injection and a reduction in injection pressure were effective in reducing the MPRR and peak in-cylinder pressure at high load operation. Nieman et al. [23] assessed the potential for the high load expansion of the NG–diesel DF-PCCI concept by the KIVA-3V code with CHEMKIN. The high load operation was expanded up to an indicated mean effective pressure (IMEP) of 2.3 MPa with the use of NG and the double injection strategy of diesel. Despite the advantages of utilizing NG in a DF-PCCI engine, the low load operation suffers from high combustion loss because of the low reactivity of the NG; this acts as a barrier to commercialization [23–26]. Nieman et al. [23] showed that high efficiency and low emissions can be attained up to 1.35 MPa IMEP in the NG–diesel DF-PCCI concept without EGR. However, the low

reactivity and slow combustion of NG increased the combustion loss at 0.4 MPa IMEP in comparison with that at the higher load. Doosje et al. [24] conducted an experimental study in a multi-cylinder engine at a load range from 0.2 to 0.9 MPa BMEP. It was found that simultaneous reduction of NO_x and PM emissions can be achieved for the load range without EGR. However, the fuel consumption increased as the load decreased due to the increased friction loss, lower combustion rate, and lower combustion efficiency. Poorghasemi et al. [25] investigated strategies for optimizing the exhaust emissions of NG–diesel DF-PCCI combustion in a light-duty diesel engine. The HC and CO emissions increased significantly with a higher NG portion because the increased NG mass in the fuel–air mixture reduced the combustion rate. The HC and CO emissions were controlled by an advanced diesel pilot start of energizing (SOE), an increase in the fraction of the diesel pilot injection quantity, a lower diesel injection pressure, and a wider diesel spray angle. Ansari et al. [26] developed empirical models through regression analysis with an experimental database to predict the performance and emissions of CDC and NG–diesel DF-PCCI modes at a load range between 0.3 and 1.2 MPa IMEP. The NG–diesel DF-PCCI mode was relatively superior in terms of operating cost and emissions, especially NO_x and PM emissions, at engine loads above 0.7 MPa IMEP. The diesel injection strategy was concentrated on HC and CO emissions at medium loads and the MPRR at higher loads. Although the DF-PCCI mode was selected at a load range between 0.7 and 1.2 MPa IMEP, the diesel CDC was the optimum combustion mode under low load conditions. Expansion to low loads was limited in the DF-PCCI mode, mainly due to the deteriorated fuel economy and high HC and CO emissions.

Despite the limitations of the NG–diesel DF-PCCI concept under low load conditions, very little research has focused on strategies for overcoming these limitations. The high levels of HC and CO emissions are mainly caused by the globally lean fuel–air mixture and its low combustion temperature under low load conditions [27]. Therefore, in the present study, an injection strategy of fuel supply, including NG and diesel, in a DF-PCCI engine under low load conditions was investigated in order to reduce both the fuel consumption and the HC and CO emissions by improving the formation of the fuel–air mixture. First, the effects of the diesel SOE and the blending ratio of NG to diesel on the combustion and emissions in the DF-PCCI engine were examined. Second, a double injection strategy of diesel was introduced in order to effectively control the fuel–air premixed mixture. Finally, different combinations of NG substitution, diesel injection strategy, and EGR were compared in order to identify a solution to the limitations of the NG–diesel DF-PCCI engine under low load conditions.

2. Experimental setup and conditions

2.1. Experimental setup

A single-cylinder diesel engine was modified to implement the DF-PCCI concept. The engine specifications are shown in Table 1.

Table 1
Engine specifications.

Item	Specification
Engine type	Single-cylinder compression-ignition
Displacement (L)	0.981
Bore (mm)	100
Stroke (mm)	125
Compression ratio	17.4
Valves per cylinder	4 (2 intake and 2 exhaust)
Fuel injection equipment	Common-rail direct-injection system
EGR system	Cooled-EGR

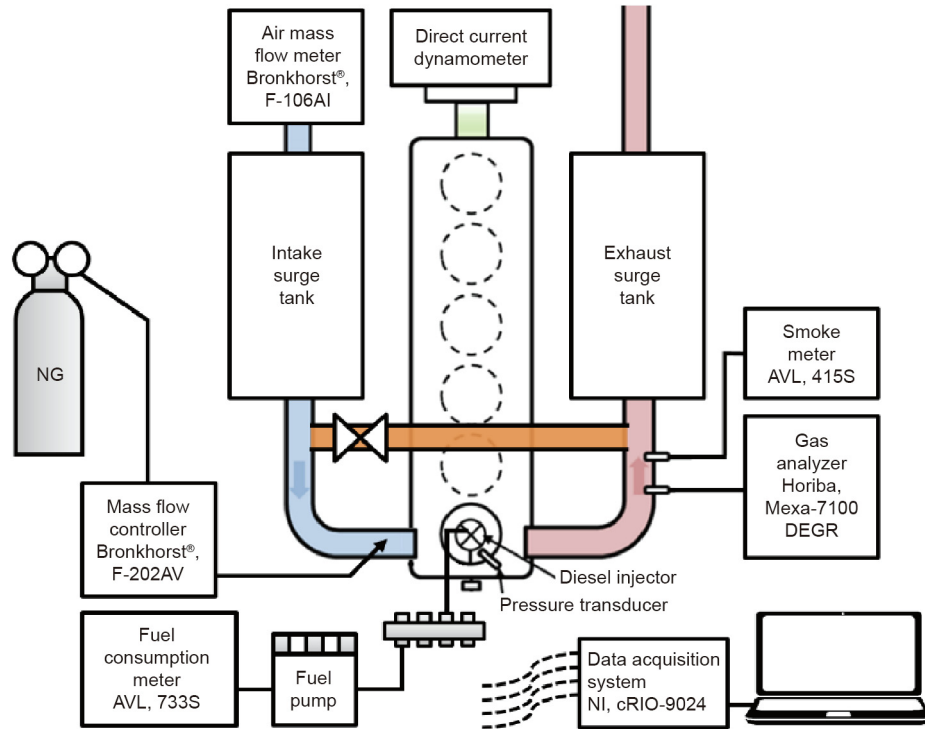


Fig. 1. Schematic diagram of experimental engine setup.

The engine had a displacement of 0.981 L and a compression ratio of 17.4. A schematic of the experimental engine setup is presented in Fig. 1. A detailed description of the experimental devices is found in a previous study by the authors [28]. NG was supplied with air during the intake stroke to create a homogeneous NG–air mixture in the cylinder. The NG mass flow rate was adjusted by an NG mass flow controller (Bronkhorst®, F-202AV), and the air mass flow rate was measured by an air mass flow meter (Bronkhorst®, F-106AI). Diesel was injected into the cylinder via a high-pressure pump and a common-rail direct-injection system. The mass flow rate of the diesel was recorded by a fuel consumption meter (AVL, 733S). The NG and diesel properties tested in this study are shown in Tables 2 and 3, respectively. The content of methane in the NG was about 91%. The motor octane number (MON) and methane number (MN) of the NG were 124 and 81.7, respectively. The diesel had a cetane number of 52.1. NG substitution was defined in this study to represent the in-cylinder fuel-blending ratio of NG to diesel. The NG substitution was determined by the energy content of NG divided by the total energy content, as shown in Eq. (1).

Table 2
Properties of NG.

Item	Value
Methane (CH ₄ , %)	91.31
Ethane (C ₂ H ₆ , %)	5.34
Propane (C ₃ H ₈ , %)	2.17
<i>i</i> -butane (<i>i</i> -C ₄ H ₁₀ , %)	0.46
<i>n</i> -butane (<i>n</i> -C ₄ H ₁₀ , %)	0.48
<i>i</i> -pentane (<i>i</i> -C ₅ H ₁₂ , %)	0.016
<i>n</i> -pentane (<i>n</i> -C ₅ H ₁₂ , %)	0.002
Nitrogen (N ₂ , %)	0.222
Reactive H/C ratio	3.78
MON	124
MN	81.7
LHV (MJ·kg ⁻¹)	46.5

MON: motor octane number; MN: methane number; LHV: lower heating value.

Table 3
Properties of diesel.

Item	Value
Density at 293 K (kg·m ⁻³)	826
Cetane number	52.1
LHV (MJ·kg ⁻¹)	42.5
T10 (K)	508
T50 (K)	562
T90 (K)	616

$$\text{NG substitution (\%)} = \frac{\dot{m}_{\text{NG}} \cdot \text{LHV}_{\text{NG}}}{\dot{m}_{\text{NG}} \cdot \text{LHV}_{\text{NG}} + \dot{m}_{\text{diesel}} \cdot \text{LHV}_{\text{diesel}}} \times 100 \quad (1)$$

where \dot{m}_{NG} and \dot{m}_{diesel} are the mass flow rates of NG and diesel, respectively, and LHV_{NG} and $\text{LHV}_{\text{diesel}}$ are the lower heating values (LHVs) of NG and diesel. The indicated thermal efficiency (ITE) in this study was obtained through Eq. (2).

$$\text{ITE (\%)} = \frac{3.6P}{\dot{m}_{\text{NG}} \cdot \text{LHV}_{\text{NG}} + \dot{m}_{\text{diesel}} \cdot \text{LHV}_{\text{diesel}}} \times 100 \quad (2)$$

where P is the power output. A piezoresistive pressure transducer (Kistler, 4045A5) and a piezoelectric pressure transducer (Kistler, 6052C) were installed to measure the intake and in-cylinder pressure, respectively. A gas analyzer (Horiba, Mexa-7100 DEGR) was used to measure the engine-out emissions, including total hydrocarbon (THC), CO, CO₂, oxygen (O₂), and NO_x. A smoke meter (AVL, 415S) was also utilized to measure the engine-out smoke emissions. A cooled-EGR system was installed between the exhaust and intake lines. Part of the hot exhaust gas flowed through an EGR cooler and an EGR valve into the intake port. The experimental data for the pressure and engine-out emissions were obtained by a data-acquisition system (NI, cRIO-9024). HRR analysis was conducted using the acquired pressure data [29]. The CA50 was defined as the crank angle where 50% of the total heat release occurs. The combustion efficiency in the study was determined by Eq. (3).

$$\text{Combustion efficiency (\%)} = \left(1 - \frac{\dot{m}_{\text{CO}} \cdot \text{LHV}_{\text{CO}} + \dot{m}_{\text{THC}} \cdot \text{LHV}_{\text{fuel}}}{\dot{m}_{\text{NG}} \cdot \text{LHV}_{\text{NG}} + \dot{m}_{\text{diesel}} \cdot \text{LHV}_{\text{diesel}}}\right) \times 100 \quad (3)$$

where \dot{m}_{CO} and \dot{m}_{THC} are the mass flow rates of CO and THC, respectively, and LHV_{CO} is the LHV of CO. It was assumed that LHV_{fuel} was calculated reflecting the ratio of NG to diesel, as shown in Eq. (4).

$$\text{LHV}_{\text{fuel}}(\text{MJ} \cdot \text{kg}^{-1}) = \frac{\dot{m}_{\text{NG}} \cdot \text{LHV}_{\text{NG}} + \dot{m}_{\text{diesel}} \cdot \text{LHV}_{\text{diesel}}}{\dot{m}_{\text{NG}} + \dot{m}_{\text{diesel}}} \quad (4)$$

2.2. Experimental conditions and test procedure

The objective of this study was to suggest an injection strategy of fuel supply, including NG and diesel, in a DF-PCCI engine under low load conditions. First, a parametric investigation with diesel SOE and NG substitution was performed to analyze the effects of the substitution on DF-PCCI combustion. The operating conditions for the parametric study are shown in Table 4. The engine was operated at a net IMEP of 0.3 MPa, which represents a low load condition. The load was kept constant during the experiment. The changes in load value according to the changes of the experimental parameters, such as the diesel injection strategy and NG substitution, were adjusted by controlling the mass flow rates of NG and diesel. The engine speed was fixed at 1400 r·min⁻¹. The NG substitution was varied from 20% to 80%, and the diesel SOE was varied from -70 to 0 crank angle degree (CAD) after top dead center (aTDC). Second, double injection strategies of diesel were introduced in order to appropriately distribute the diesel spray in the combustion chamber. The diesel main SOE was selected based on the parametric study. The diesel pilot SOE and the fraction of the diesel pilot injection quantity were varied to control the reactivity of the fuel–air mixture. An external cooled EGR was introduced to retard the combustion phasing of the DF-PCCI combustion toward top dead center (TDC). Finally, different combinations of NG substitution, diesel injection strategy, and EGR were compared. It should be noted that NO_x and PM emissions were limited to below the Euro VI regulation (NO_x < 0.4 g·(kW·h)⁻¹, PM < 0.01 g·(kW·h)⁻¹) during the experimental tests. Misfire in this

study was defined as a coefficient of variation of an IMEP value higher than 5%.

3. Results and discussion

3.1. Effect of diesel SOE and NG substitution

This section describes the effects of diesel SOE and NG substitution on the combustion and emissions in the NG–diesel DF-PCCI engine for the low load. The diesel SOE was varied from -70 to 0 CAD aTDC in increments of 5 CAD, and the NG substitution was varied from 20% to 80% in increments of 20%. Fig. 2 shows the ITE and CA50 for the NG substitution and diesel SOE. A region of high efficiency was located at the diesel SOE between -40 and -30 CAD aTDC and the NG substitution between 40% and 60%. The region corresponded to a “sweet spot” for diesel SOEs, CA50 locations near TDC, and moderate NG substitutions. The diesel spray reached both the squish and piston bowl regions at the diesel SOEs, which increased the reactivity of the fuel–air mixture in these regions [28]. When the diesel SOE was advanced and the NG substitution was reduced further outside of the high ITE region, the ITE deteriorated significantly. When the diesel was injected between -15 and -10 CAD aTDC, the ITE was comparable to that of the high-efficiency region with an NG substitution of 20% to 40%. However, when the NG substitution was higher than 60%, the ITE deteriorated rapidly. The higher NG substitution under the low load condition caused a globally leaner fuel–air mixture, which resulted in low combustion efficiency and thermal efficiency [30]. When the diesel was injected near TDC, the combustion phasing depended on the diesel SOE. For example, the combustion phasing was retarded toward TDC as the diesel SOE was retarded, which is known as diffusive dual-fuel combustion [20,27]. However, when the diesel SOE was advanced before -25 CAD aTDC, the combustion phasing was moved toward TDC by advancing the diesel SOE and increasing the NG substitution, which is known as premixed RCCI combustion [21–26]. The retardation of the combustion phasing was due to the formation of a locally lower reactivity fuel–air mixture at the start of combustion (SOC) with a higher NG substitution and an advanced diesel SOE [22]. Although advancing the diesel SOE and increasing the NG substitution were beneficial for controlling the combustion phasing location, the probability of incomplete combustion—or even misfire—also increased. It should be noted that the misfire zones are located in the upper left and upper right regions shown in Fig. 2. This is because the fuel–air mixture was over-lean under the low load condition, so the mixture was near the lean flammability limit. The advanced diesel SOE and increased NG substitution intensified the reduction in the local reactivity of the fuel–air mixture. Therefore, the area of misfire in Fig. 2 increased with an advanced diesel

Table 4
Operating conditions for a parametric study with diesel SOE and NG substitution.

Item	Condition
Engine load (MPa net IMEP)	0.3
Engine speed (r·min ⁻¹)	1400
Intake temperature (K)	300 ± 1
Coolant temperature (K)	353 ± 1
Diesel injection pressure (MPa)	100
NG substitution (%)	20 to 80 (increment of 20)
Diesel SOE (CAD aTDC)	-70 to 0 (increment of 5)

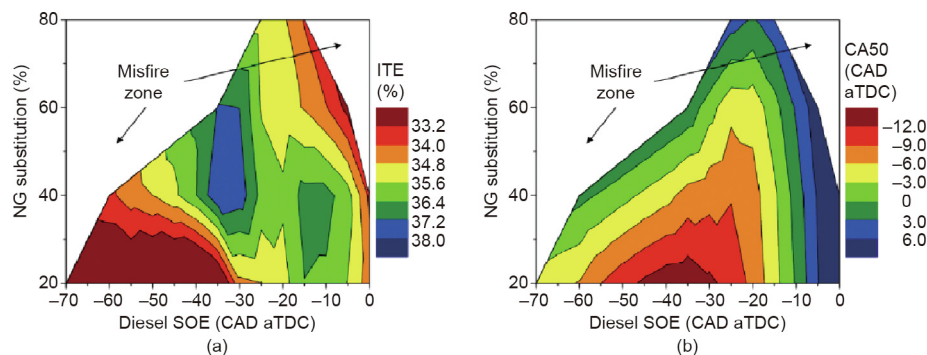


Fig. 2. (a) ITE and (b) CA50 according to NG substitution and diesel SOE.

SOE and a higher NG substitution. Figs. 3 and 4 show the NO_x , PM, THC, and CO emissions according to the diesel SOE and NG substitution. The NO_x and PM emissions decreased when the diesel SOE was advanced and the NG substitution was increased, whereas the THC and CO emissions increased. This finding could be explained by the HRR curves in Fig. 5. The combustion phasing was retarded with a lower peak HRR when an advanced diesel SOE and higher NG substitution were applied. This result occurred because the fuel–air mixture had lower reactivity at the SOC and reduced the combustion temperature, which resulted in low NO_x and PM emissions at the expense of increased THC and CO emissions. Although the THC emissions were dependent on both NG substitution and diesel SOE, the parameter with a dominant influence on the THC emissions differed according to the diesel SOE. When the diesel

was injected before -40 CAD aTDC, the diesel SOE had greater influence on the THC emissions than the NG substitution. However, the NG substitution played a more dominant role on the THC emissions than the diesel SOE when the diesel was injected after -40 CAD aTDC. In this test, a homogeneous NG–air mixture was formed at the SOC because the NG was introduced into the combustion chamber during the intake stroke. Part of the mixture was not involved in the combustion because the mixture was trapped in crevices [28]. Although the mixture flowed back into the combustion chamber during the expansion stroke, the combustion temperature was too low to oxidize the mixture under the low load operation. Therefore, when the NG substitution increased for the low load, the trapped NG increased and was mostly emitted as THC emissions. In addition to the trapped NG, a lower combustion

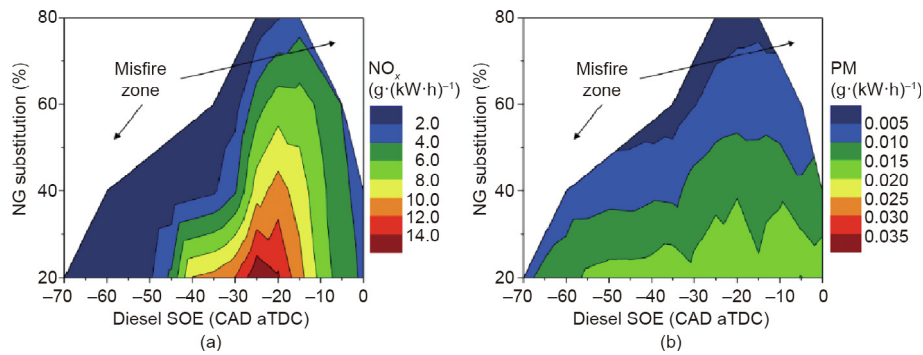


Fig. 3. (a) NO_x and (b) PM emissions according to NG substitution and diesel SOE.

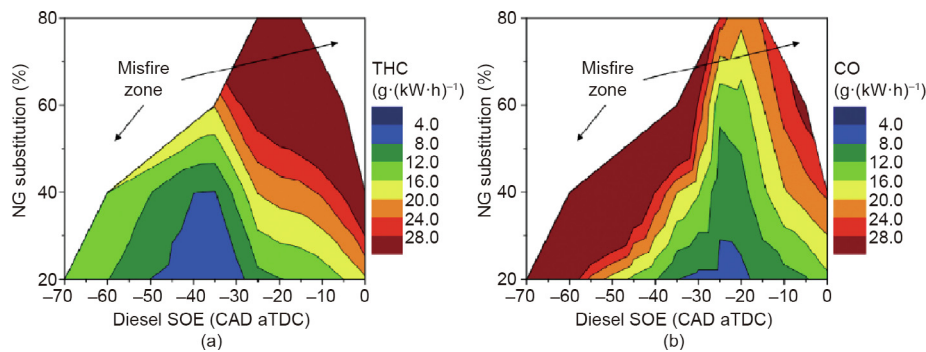


Fig. 4. (a) THC and (b) CO emissions according to NG substitution and diesel SOE.

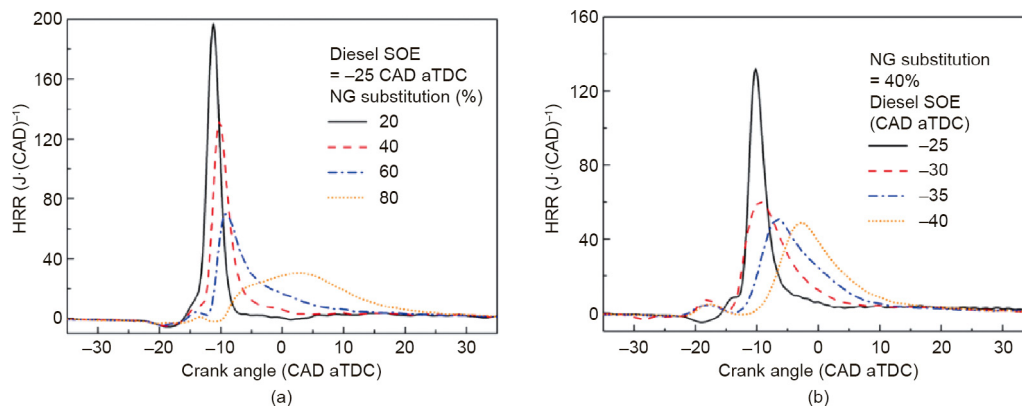


Fig. 5. HRR curves according to (a) NG substitution and (b) diesel SOE.

temperature also resulted in increased THC emissions as the NG substitution was increased. Based on the performance and exhaust gas emissions results, the points that combined high efficiency with low exhaust emissions occurred at either an NG substitution of 40% and a diesel SOE of –35 CAD aTDC, or an NG substitution of 60% and a diesel SOE of –30 CAD aTDC. Therefore, these points were selected as the baseline of the NG–diesel DF-PCCI combustion in this study.

3.2. Effect of the diesel injection strategy and cooled EGR

Double injection strategies of direct-injected diesel have been shown to be effective for appropriately distributing the fuel in the cylinder of a DF-PCCI engine, as well as for controlling the local reactivity of the premixed fuel–air mixture [15]. In this section, the effects of a diesel pilot SOE and the fraction of the diesel pilot injection quantity on NG–diesel DF-PCCI combustion were investigated. Table 5 lists the operating conditions for the double injection strategy of diesel. The double injection strategy was applied to NG substitutions of both 40% and 60%, which were selected as the baseline points for the DF-PCCI engine, as mentioned in the previous section. The diesel main SOEs of the NG substitutions of 40% and 60% were –35 and –30 CAD aTDC, respectively. The diesel pilot SOE was varied in increments of 5 CAD, and the fraction of diesel pilot injection quantity was varied in increments of 10%. The minimum dwell time between the pilot and main injection of diesel was 5 CAD to avoid interference between the two injections. The experimental results for the NG substitution of 40% are given in this section, since the effects of the double injection strategy on the DF-PCCI combustion were similar. Figs. 6 and 7 show the performance and exhaust emissions according to the pilot SOE and pilot injection quantity of diesel, respectively. The ITE of the diesel double injection was higher than that of the single injection because of the retarded combustion phasing. The implementation of the pilot injection, which was injected before the main injection, reduced the main injection quantity. Therefore, the application of the pilot injection reduced the reactivity of the fuel–air mixture and retarded the combustion phasing. As the diesel pilot SOE was advanced, the ITE was comparatively reduced, despite the slightly retarded combustion phasing toward TDC. The advanced pilot injection reduced the reactivity of the mixture, which reduced the combustion temperature and thus lowered the combustion efficiency, as shown in Fig. 8. Therefore, additional NG and diesel were introduced to compensate for the lower power. Although the advanced pilot injection was favorable for simultaneously reducing NO_x and PM emissions, the THC and CO emissions were worse because of the lower combustion temperature. Therefore, the retarded diesel pilot SOE was selected based on the relatively improved ITE, THC, and CO emissions, which were the main objective of this research. The fraction between the pilot injection and the main injection of diesel was also varied in order to form a favorable mixture for DF-PCCI combustion, as shown in Fig. 7. As the fraction of the diesel pilot injection quantity increased, the ITE decreased, despite the slightly retarded combustion phasing, because of the lower combustion efficiency, as shown in Fig. 8. A

Table 5
Operating conditions for a double injection strategy of diesel.

Item	NG substitution of 40%	NG substitution of 60%
Diesel main SOE (CAD aTDC)	–35	–30
Diesel pilot SOE (CAD aTDC)	–55 to –40	–50 to –35
Fraction of diesel pilot injection quantity (%)	20 to 50	20 to 50

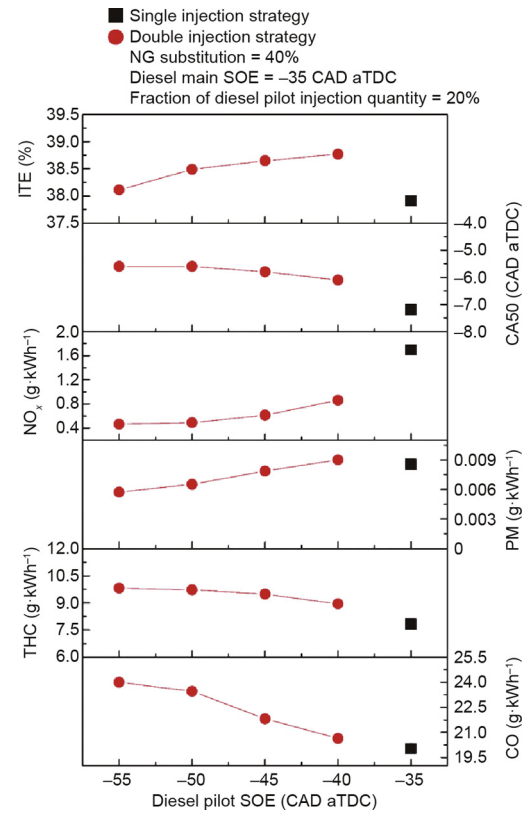


Fig. 6. Performance and exhaust gas emissions according to diesel pilot SOE.

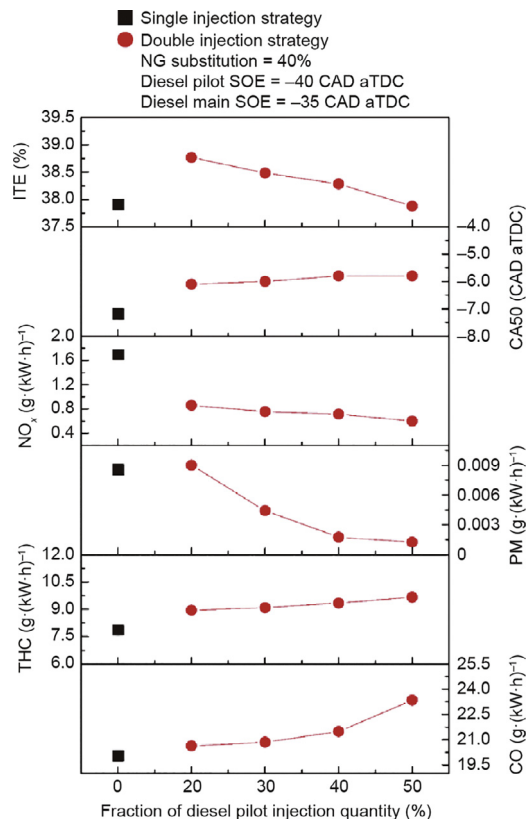


Fig. 7. Performance and exhaust gas emissions according to the fraction of diesel pilot injection quantity.

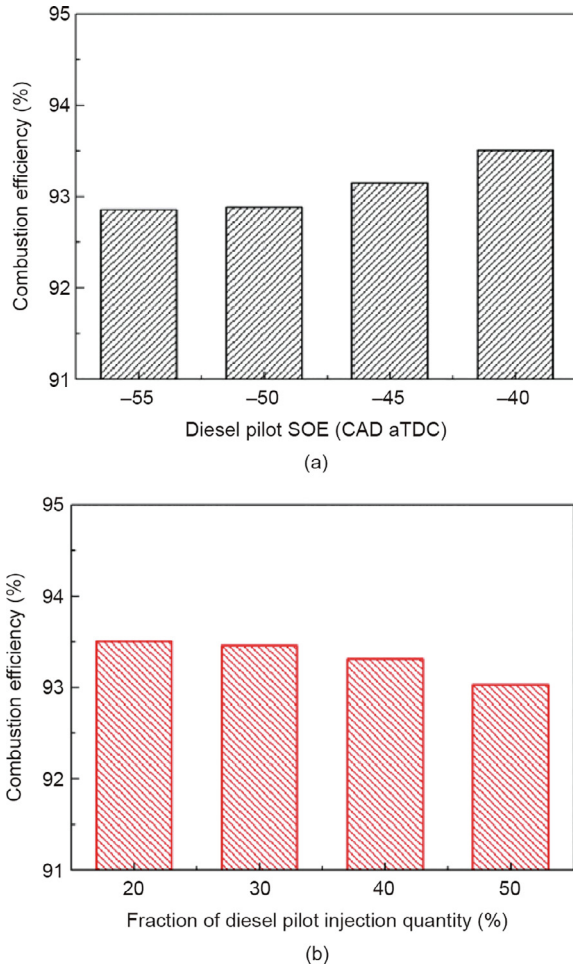


Fig. 8. Combustion efficiency according to (a) diesel pilot SOE and (b) fraction of diesel pilot injection quantity.

higher fraction of the diesel pilot injection quantity meant that a lower quantity of the main injection was introduced into the combustion chamber. Therefore, the fuel–air mixture had a lower reactivity, which deteriorated the combustion efficiency. A higher fraction of the diesel pilot injection quantity produced effects similar to those of the advanced diesel pilot SOE. Based on the results above, a retarded diesel pilot SOE and lower fraction of the diesel pilot injection quantity were favorable for improving the ITE, THC, and CO emissions. In other words, stratifying the fuel–air mixture was more effective than increasing the homogeneity of the fuel–air mixture under the low load condition, which formed an over-lean fuel–air mixture. Despite the implementation of double injection strategies, the DF-PCCI combustion showed quite advanced combustion phasing and high NO_x emissions. Therefore, cooled EGR was introduced to retard the combustion phasing and reduce the NO_x emissions. Fig. 9 shows the performance and exhaust emissions according to the EGR rate. When the EGR rate was increased to 25%, the ITE improved due to the retardation of combustion phasing toward TDC. When CA50 is located before TDC, the negative work reduces the ITE [3]. The introduction of the EGR up to 25% retarded the CA50 toward TDC and improved the ITE. However, further increase of the EGR rate reduced the ITE, mainly because of the abrupt reduction of combustion efficiency. Fig. 10 shows the HRR curves according to the EGR rate. As the EGR rate was increased, the peak of the HRR decreased and the combustion duration increased, causing a lower

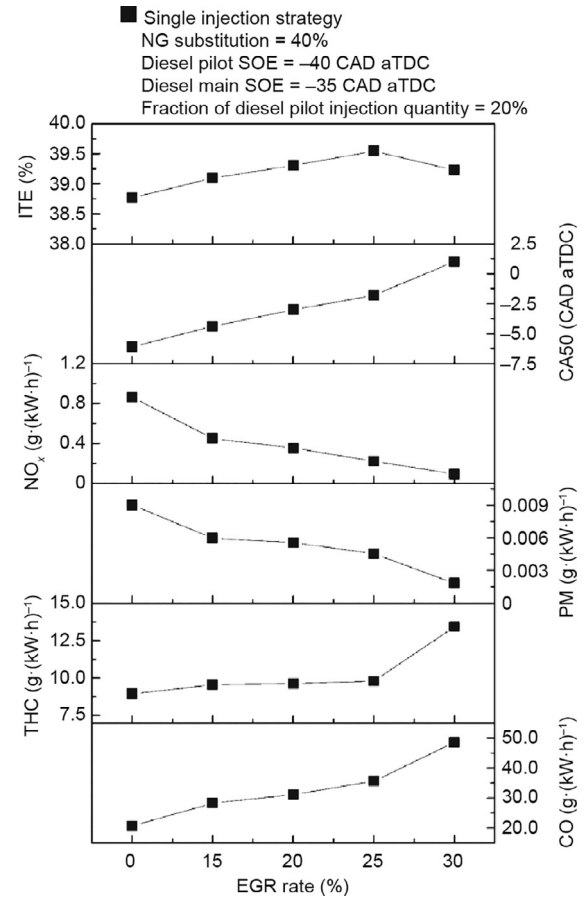


Fig. 9. Performance and exhaust gas emissions according to EGR rate.

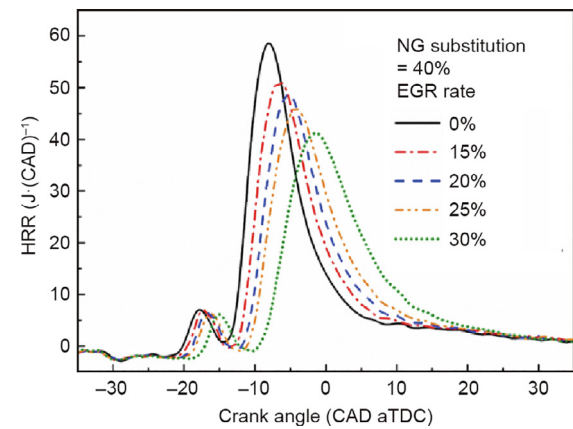


Fig. 10. HRR curves according to EGR rate.

peak combustion temperature; this sharply reduced the NO_x and PM emissions at the expense of increased CO emissions. The dilution, thermal, and chemical effects of the cooled EGR lowered the combustion temperature and contributed to the low NO_x and PM emissions [31,32]. The THC emissions increased slightly up to an EGR rate of 25%; however, the emissions jumped at an EGR rate of 30% due to incomplete combustion. The NO_x and PM emissions were kept below the Euro VI regulation by implementing the cooled EGR. The best indicated efficiency was achieved with an EGR rate of 25% at the expense of increased CO emissions.

3.3. Operating strategy for DF-PCCI combustion under low load conditions

In this section, different combinations of NG substitution, diesel injection strategy, and EGR are compared in order to identify a solution to the issue of low load operation in NG–diesel DF-PCCI combustion. Fig. 11 compares the NG substitutions of 40% and 60% in terms of performance and exhaust gas emissions. It is notable that the result of the diesel injection strategy with an NG substitution of 60% was similar to that with an NG substitution of 40%, as described in Section 3.2, which stratified the fuel–air mixture with a retarded diesel pilot SOE and a lower fraction of the diesel pilot injection quantity. However, relatively retarded double injection timings were applied with the NG substitution of 60% in order to compensate for the reduction in the local equivalence ratio and reactivity of the fuel–air mixture in comparison with those with an NG substitution of 40%. The best ITE in the NG substitution of 60% was achieved at an EGR rate of 15%, whereas the EGR rate that achieved the best ITE in the NG substitution of 40% was 25%. Despite the different EGR ratios, the location of CA50 corresponding to the best ITE was similar with both NG substitutions. The ITE for the NG substitution of 60% was lower than that for the NG substitution of 40%. The lower ITE for the NG substitution of 60% can be explained by the shape of the HRR curve and the combustion efficiency, as shown in Figs. 12 and 13. Fig. 12 shows the HRR curves of the applied NG substitutions at a fixed CA50. It is notable that a lower EGR rate was needed for the higher NG substitution in

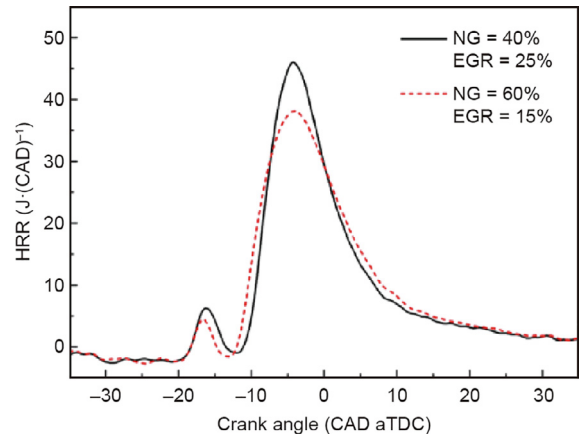


Fig. 12. HRR curves for the NG substitutions of 40% and 60%.

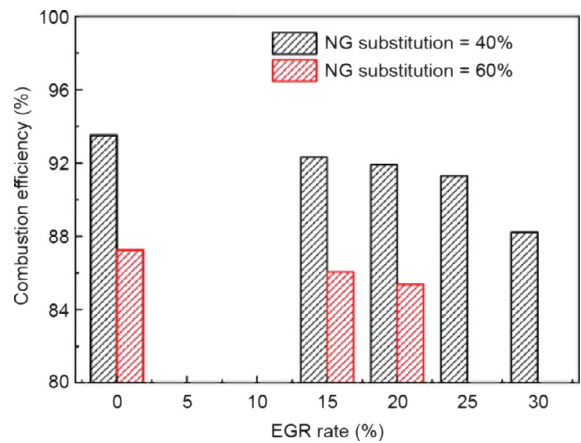


Fig. 13. Combustion efficiencies for the NG substitutions of 40% and 60%.

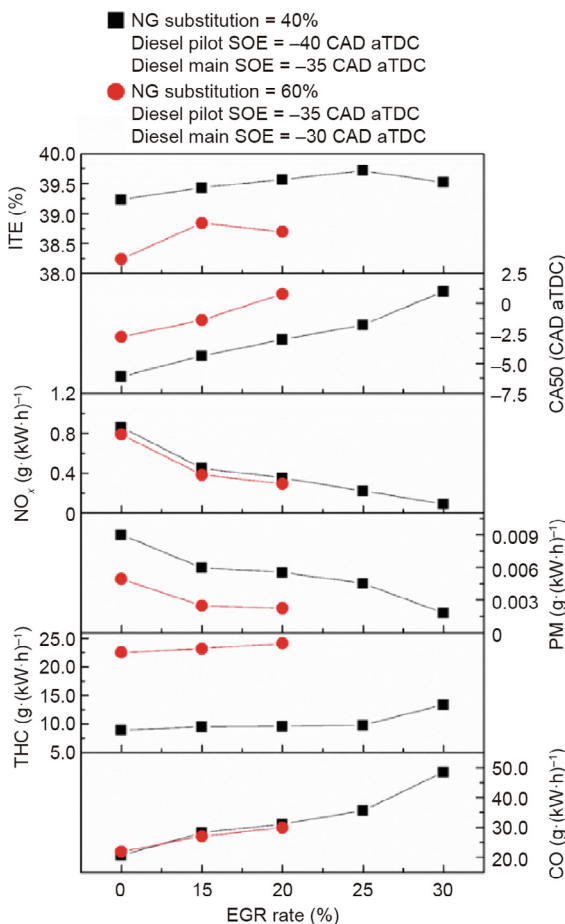


Fig. 11. Comparisons between the NG substitutions of 40% and 60% in terms of performance and exhaust gas emissions.

order to keep the CA50 constant. In other words, the same CA50 could be achieved with an EGR rate of 15% for the NG substitution of 60%, but the EGR rate was 25% for the NG substitution of 40%. The combustion at a higher NG substitution showed a lower peak of HRR and increased combustion duration, which was not favorable for thermal efficiency [33]. In general, as a higher NG substitution is applied, the peak HRR increases at the same CA50. This is because the increase in the NG substitution leads to an enhancement of the homogeneous fuel–air mixture [12]. However, this trend was reversed in the present study. As the NG substitution was increased from 40% to 60%, the peak HRR was reduced. In this study, the engine was operated at 0.3 MPa net IMEP, which resulted in an overly lean fuel–air mixture. In this situation, as the NG substitution was increased, the NG reduced the rate of combustion and the peak HRR [25,28]. Fig. 13 shows the combustion efficiencies of both NG substitutions according to the EGR rate. The combustion loss for the NG substitution of 60% was significantly higher than that for the NG substitution of 40%. The mass of NG trapped in crevices, which was not involved in the combustion, increased with higher NG substitution. Therefore, the combustion efficiency was reduced and the THC emissions increased rapidly with the higher NG substitution.

Table 6 summarizes the main results of the NG substitution of 40% and 60%. The ITE for the NG substitution of 40% increased by 3.7% in comparison with that for the NG substitution of 60%. The

Table 6
Comparison between the NG substitution of 40% and 60%.

Item	NG substitution of 40%	NG substitution of 60%
ITE (%)	39.5	38.1
CA50 (CAD aTDC)	−1.8	−1.6
Combustion efficiency (%)	91.3	86.1
NO _x emissions (g·(kW·h) ^{−1})	0.22	0.38
PM emissions (g·(kW·h) ^{−1})	0.0045	0.0025
THC emissions (g·(kW·h) ^{−1})	9.8	23
CO emissions (g·(kW·h) ^{−1})	36	27

higher ITE for the lower NG substitution was due to the higher combustion efficiency and the increased combustion rate with the higher peak HRR. The NO_x and PM emissions were below the Euro VI regulation in both NG substitutions. The THC emissions for the NG substitution of 40% decreased by 57% in comparison with those for the NG substitution of 60%, while the CO emissions increased by 33%. Based on the results, the success of implementing a higher NG substitution for the low load was limited, mainly because of a higher fuel consumption and higher THC emissions.

4. Conclusions

In this study, an injection strategy of fuel supply, including NG and diesel, was investigated in a DF-PCCI engine in order to reduce the fuel consumption and HC and CO emissions under low load conditions. The major findings can be summarized as follows:

- The formation of a fuel–air mixture was effectively controlled by a variation in the NG substitution and diesel SOE. The HC and CO emissions increased significantly when the diesel SOE was advanced and the NG substitution was increased, because the reactivity of the fuel–air mixture was reduced.
- When the double injection strategy of diesel was implemented in the DF-PCCI combustion, retarding a diesel pilot SOE and a low fraction of the diesel pilot injection quantity were favorable for the simultaneous reduction of fuel consumption, HC emissions, and CO emissions. In other words, stratification of the fuel–air mixture was more desirable than an increased homogeneity of the mixture for the low load condition.
- The introduction of EGR effectively improved the fuel economy and reduced the NO_x and PM emissions under the Euro VI regulation by retarding the combustion phasing.
- The implementation of a higher NG substitution for the low load operation showed limited success, mainly because of higher HC emissions and a higher fuel consumption.

Based on the experimental results, the combination of an NG substitution of 40%, the double injection strategy of diesel, and a moderate EGR rate effectively reduced the HC and CO emissions and improved the combustion efficiency and indicated efficiency under the low load condition of DF-PCCI combustion.

Acknowledgement

The authors would like to express their appreciation for the Global-Top Project, Development of Advanced Combustion Technology for Global Top Low Emission Vehicle (2016002070001), of the Ministry of Environment (MOE) of Korea for financial support by the Center for Environmentally Friendly Vehicle (CEFV). The authors would also like to thank Zenobalti Co. for their technical support.

Compliance with ethics guidelines

Hyunwook Park, Euijoon Shim, and Choongsik Bae declare that they have no conflict of interest or financial conflicts to disclose.

Nomenclature

aTDC	after top dead center
BMEP	brake mean effective pressure
CAD	crank angle degree
CDC	conventional diesel combustion
CO	carbon monoxide
CO ₂	carbon dioxide
DF-PCCI	dual-fuel premixed charge compression ignition
EGR	exhaust gas recirculation
HC	hydrocarbon
HRR	heat-release rate
IMEP	indicated mean effective pressure
ITE	indicated thermal efficiency
LHV	lower heating value
MN	methane number
MON	motor octane number
MPRR	maximum pressure rise rate
NG	natural gas
NO _x	nitrogen oxides
PCCI	premixed charge compression ignition
PM	particulate matter
RCCI	reactivity-controlled compression ignition
SOC	start of combustion
TDC	top dead center
THC	total hydrocarbon
\dot{m}	mass flow rate

References

- [1] US Energy Information Administration (EIA). Annual energy outlook with projects to 2050. Washington, DC: EIA; 2017.
- [2] Yao M, Zheng Z, Liu H. Progress and recent trends in homogeneous charge compression ignition (HCCI) engines. *Pror Energy Combust Sci* 2009;35(5):398–437.
- [3] Saxena S, Bedoya ID. Fundamental phenomena affecting low temperature combustion and HCCI engines, high load limits and strategies for extending these limits. *Pror Energy Combust Sci* 2013;39(5):457–88.
- [4] Agarwal AK, Singh AP, Maurya RK. Evolution, challenges and path forward for low temperature combustion engines. *Pror Energy Combust Sci* 2017;61:1–56.
- [5] Liu MB, He BQ, Zhao H. Effect of air dilution and effective compression ratio on the combustion characteristics of a HCCI (homogeneous charge compression ignition) engine fuelled with *n*-butanol. *Energy* 2015;85:296–303.
- [6] Paykani A, Kakaee AH, Rahnama P, Reitz RD. Progress and recent trends in reactivity-controlled compression ignition engines. *Int J Engine Res* 2016;17(5):481–524.
- [7] Inagaki K, Fuyuto T, Nishikawa K, Nakakita K, Sakata I. Dual-fuel PCI combustion controlled by in-cylinder stratification of ignitability. SAE technical paper. Washington, DC: SAE International; 2006. No.: 2006-01-0028.
- [8] Kokjohn SL, Hanson RM, Splitter DA, Reitz RD. Experiments and modeling of dual-fuel HCCI and PCCI combustion using in-cylinder fuel blending. *SAE Int J Engines* 2009;2:24–39.
- [9] Benajes J, Molina S, García A, Monsalve-Serrano J. Effects of direct injection timing and blending ratio on RCCI combustion with different low reactivity fuels. *Energy Convers Manage* 2015;99:193–209.
- [10] Ma S, Zheng Z, Liu H, Zhang Q, Yao M. Experimental investigation of the effects of diesel injection strategy on gasoline/diesel dual-fuel combustion. *Appl Energy* 2013;109:202–12.
- [11] Wang Y, Zhu Z, Yao M, Li T, Zhang W, Zheng Z. An investigation into the RCCI engine operation under low load and its achievable operational range at different engine speeds. *Energy Convers Manage* 2016;124:399–413.
- [12] Wang Y, Yao M, Li T, Zhang W, Zheng Z. A parametric study for enabling reactivity controlled compression ignition (RCCI) operation in diesel engines at various engine loads. *Appl Energy* 2016;175:389–402.
- [13] Benajes J, Pastor JV, García A, Monsalve-Serrano J. The potential of RCCI concept to meet Euro VI NO_x limitation and ultra-low soot emissions in a heavy-duty engine over the whole engine map. *Fuel* 2015;159:952–61.

- [14] Kokjohn SL, Hanson RM, Splitter DA, Reitz RD. Fuel reactivity controlled compression ignition (RCCI): a pathway to controlled high-efficiency clean combustion. *Int J Engine Res* 2011;12(3):209–26.
- [15] Splitter D, Hanson R, Kokjohn S, Wissink M, Reitz RD. Injection effects in low load RCCI dual-fuel combustion. SAE technical paper. Washington, DC: SAE International; 2011. No.: 2011-24-0047.
- [16] Molina S, García A, Pastor JM, Belarte E, Balloul I. Operating range extension of RCCI combustion concept from low to full load in a heavy-duty engine. *Appl Energy* 2015;143:211–27.
- [17] Hanson R, Ickes A, Wallner T. Comparison of RCCI operation with and without EGR over the full operating map of a heavy-duty diesel engine. SAE technical paper. Washington, DC: SAE International; 2016. No.: 2016-01-0794.
- [18] Tong L, Wang H, Zheng Z, Reitz R, Yao M. Experimental study of RCCI combustion and load extension in a compression ignition engine fueled with gasoline and POGE. *Fuel* 2016;181:878–86.
- [19] Jia Z, Denbratt I. Experimental investigation of natural gas-diesel dual-fuel RCCI in a heavy-duty engine. *SAE Int J Engines* 2015;8:797–807.
- [20] Dahodwala M, Joshi S, Koehler EW, Franke M. Investigation of diesel and CNG combustion in a dual fuel regime and as an enabler to achieve RCCI combustion. SAE technical paper. Washington, DC: SAE International; 2014. No.: 2014-01-1308.
- [21] Walker NR, Wissink ML, DelVescovo DA, Reitz RD. Natural gas for high load dual-fuel reactivity controlled compression ignition in heavy-duty engines. *J Energy Resour Technol* 2015;137(4):042202.
- [22] Dahodwala M, Joshi S, Koehler E, Franke M, Tomazic D. Experimental and computational analysis of diesel-natural gas RCCI combustion in heavy-duty engines. SAE technical paper. Washington, DC: SAE International; 2015. No.: 2015-01-0849.
- [23] Nieman DE, Dempsey AB, Reitz RD. Heavy-duty RCCI operation using natural gas and diesel. *SAE Int J Engines* 2012;5:270–85.
- [24] Doosje E, Willems F, Baert R. Experimental demonstration of RCCI in heavy-duty engines using diesel and natural gas. SAE technical paper. Washington, DC: SAE International; 2014. No.: 2014-01-1318.
- [25] Poorghasemi K, Saray RK, Ansari E, Irdmouza BK, Shahbakhti M, Naber JD. Effect of diesel injection strategies on natural gas/diesel RCCI combustion characteristics in a light duty diesel engine. *Appl Energy* 2017;199:430–46.
- [26] Ansari E, Shahbakhti M, Naber J. Optimization of performance and operational cost for a dual mode diesel-natural gas RCCI and diesel combustion engine. *Appl Energy* 2018;231:549–61.
- [27] Wei L, Geng P. A review on natural gas/diesel dual fuel combustion, emissions and performance. *Fuel Process Technol* 2016;142:264–78.
- [28] Park H, Shim E, Bae C. Improvement of combustion and emissions with exhaust gas recirculation in a natural gas-diesel dual-fuel premixed charge compression ignition engine at low load operations. *Fuel* 2019;235:763–74.
- [29] Heywood JB. *Internal combustion engine fundamentals*. New York: McGraw-hill; 1988.
- [30] Khatamnejad H, Khalilarya S, Jafarmadar S, Mirsalim M, Dahodwala M. Influence of blend ratio and injection parameters on combustion and emissions characteristics of natural gas-diesel RCCI engine. SAE technical paper. Washington, DC: SAE International; 2017. No.: 2017-24-0083.
- [31] Al-Qurashi K, Lueking AD, Boehman AL. The deconvolution of the thermal, dilution, and chemical effects of exhaust gas recirculation (EGR) on the reactivity of engine and flame soot. *Combust Flame* 2011;158(9):1696–704.
- [32] Fathi M, Saray RK, Checkel MD. The influence of exhaust gas recirculation (EGR) on combustion and emissions of *n*-heptane/natural gas fueled homogeneous charge compression ignition (HCCI) engines. *Appl Energy* 2011;88(12):4719–24.
- [33] Park H, Kim J, Bae C. Effects of hydrogen ratio and EGR on combustion and emissions in a hydrogen/diesel dual-fuel PCCI engine. SAE technical paper. Washington, DC: SAE International; 2015. No.: 2015-01-1815.